ORIGINAL PAPER

RJME
Romanian Journal of Morphology & Embryology
http://www.rjme.ro/

Particular molecular and ultrastructural aspects in invasive mammary carcinoma

CORINA ELENA MIHALCEA[1)], ANA-MARIA MOROŞANU[2)], DANIELA MURĂRAŞU[1)], LILIANA PUIU[1)], SABIN CINCA[1)], SILVIU CRISTIAN VOINEA[1)], NICOLAE MIRANCEA[2)]

[1)] *"Prof. Dr. Alexandru Trestioreanu" Oncological Institute, Bucharest, Romania*

[2)] *Institute of Biology Bucharest of Romanian Academy*

Abstract

Electron microscopic investigations of invasive mammary carcinoma tumors revealed that intercellular junctions, namely desmosomes are severely altered; some desmosomes became internalized. Tumor cells, especially by their invadopodia, generate and disseminate membrane vesicles, including exosomes, inside of peritumoral stroma. Telocytes, a new described interstitial/stromal cell phenotype, considered to play important roles in cell signaling, exhibited a reduced number of hetero-cellular contacts, which suggests a possible perturbation of tissular homeostasis modulation. Signaling PIK3/Akt pathway plays an important role both in carcinogenesis and in proliferation, differentiation, and cell survival. Alteration of this pathway has been observed in many human cancers, often involving an increase in the activity of PIK3CA, p110α catalytic subunit of PI3K. Our study confirms the high prevalence of PIK3CA mutations in breast cancer. In accordance with the results of the largest previous studies, 87.5% of mutations detected by DNA direct sequencing were hot spot mutations, most of them located in the kinase domain. High percentage of mutations detected by high-resolution melting makes the assay an attractive choice for mutation scanning, especially, in samples with low percentage of tumor cell.

Keywords: invasive mammary carcinoma, shedding membrane vesicles, telocytes, mutations in exons 9 and 20 of PIK3CA gene.

Introduction

Breast cancer (malignant breast neoplasm) is a disease of mammals, human being mostly affected. Women breast cancer is 100 times more common than breast cancer in man. Breast cancer is the most common form of cancer among women in Europe, USA and Canada. Distal metastasis of highly invasive breast cancer cells represents the major cause of death in the women with breast cancer [1]. Despite early detection methods and advanced conventional treatments, still there is a high rate of mortality. About 400 000 people worldwide are killed annually by breast cancer.

In case of normal human breast, the mammary tissue is represented by (1) epithelia organized as ducts, ductules and lobules and (2) stroma represented by connective tissue (mostly fibroblasts), including adipose tissue as mammary fat pad as well other resident and transitory cell types. Cancers originating from lobules are known as lobular carcinoma, while those originating from ducts are termed as ductal carcinomas. Most breast cancers are ductal carcinomas: (1) ductal carcinoma *in situ* (DCIS), also known as intraductal carcinoma, and (2) the more aggressive invasive ductal carcinoma, which has the potential to undergo metastasis. There are few treatment options: (a) surgical removal of the tumor and associated tumor tissue, (b) surgical removal of the whole breast (mastectomy), (c) chemotherapy, (d) chemo-radiotherapy, (e) hormone therapy. Both lobular and ductal epithelia can be involved in breast cancer initiation and development, including secondary formation (metastasis).

Like other cancer types, breast cancer occurs because of the permanent alterations in some genes of an individual or a group of cells. Gene mutations can be inborn or acquired along the time [2]. The most frequent genetic alterations in breast cancer involved BRCA1 and BRCA2 genes but also tumor suppressor gene PTEN loss and PIK3CA mutations occur [3].

PIK3CA gene is located in chromosomal region 3q25-27 and is composed of 20 exons coding for the p110α catalytic subunit of PI3K. According to some studies, this gene is mutated in different cancers such as glioblastoma, gastric cancer, hepatocellular carcinoma, endometrial, etc. [4]. In breast carcinomas, PIK3CA mutations occur with a frequency in a range from 16.4% to 45% [4–6]. PIK3CA mutations are found mainly in regions of exon 9 (helical domain) and exon 20 (kinase domain). The most common missense mutations of this gene results in the replacement of amino acid residues E542, and E545 with lysine in the helical domain and H1047 with arginine in kinase domain. It is noted that these mutations lead to an increased activity of PI3K [7, 8]. In primary breast tumors, mutations in the PIK3CA gene have been associated with lymph node metastasis, the presence of estrogen and progesterone receptor and overexpression of HER2 gene [3, 9]. Somatic mutations in the PIK3CA are associated with poor response to lapatinib and trastuzumab therapy, as well as the inactivation of PTEN in the cancers with HER2 gene overexpressing [10, 11].

PIK3CA is a component of PI3K heterodimer consisting in two subunits: a regulatory subunit (p85) of 85 kDa and a catalytic subunit of 110 kDa. PI3K converts phosphatidylinositol-4,5-bisphosphate (PP2) to phosphatidylinositol-3,4,5-trisfosfat (PP3) on the inside of the cell membrane. Phosphatidylinositol-3-kinases (PI3K) are a group of lipid kinases that plays a role in regulation of

cell signaling pathways involved in proliferation, adhesion, survival, cell motility and neoplasia [12, 13].

PI3K is a major signal in PIK3/Akt pathway, located downstream of the epidermal growth factor receptor (HER2), and from others tyrosine kinases receptors. Molecular alterations in the signaling pathway occur in 30% of invasive breast tumors. PI3K activates AKT, SGK, PDK1 and several molecules involved in cell cycle progression and survival. PI3K/AKT pathway hyperactivation is generated by several mechanisms: PIK3CA gene mutations, AKT1 mutations, amplifications AKT2 or loss of PTEN phosphatase activity [14].

In the ER-positive breast tumors, activation of PI3K confers resistance to radiotherapy, anti-estrogen and anti-HER2 therapy. Studies concerning anti-ER and anti-HER2 therapy resistance showed drug resistance could be overcome by pharmacological inhibition of signaling pathway PIK3/AKT. It has also been shown that combination of anti-HER2 or anti-ER drugs and inhibitors of PI3K/AKT pathway may be effective strategy in the management of breast cancer HER2+ and ER+ when standard therapies did not achieve satisfactory results [15].

Establishing the diagnosis and appropriate therapeutic protocol in breast carcinoma involves extensive knowledge of ultrastructural and genetic characteristics of the tumor cell. In this study, we used electron microscopy techniques and mutation analysis methods for PIK3CA gene in order to characterize invasive breast carcinomas.

Materials and Methods

Normal and tumor tissue samples (21 pairs) were obtained from patients suffering from mammary carcinoma and surgically treated at the Department of Surgery, "Prof. Dr. Alexandru Trestioreanu" Oncological Institute, Bucharest, Romania. Informed consent was obtained from all patients enrolled. Human breast cancer cell lines were used as positive and negative controls in mutational studies. MCF7 (heterozygous for exon 9 E545K mutation), T47D (heterozygous for exon 20 H1047R mutation) and SKBR3 (wild type) cell lines were kindly donated by Dr. Irina Lorelei Braşoveanu ("Victor Babeş" National Institute for Research and Development in Pathology and Biomedical Sciences, Bucharest).

Genomic DNA was extracted from fresh tissues and breast cancer cell lines using the QIAamp DNA Mini kit (Qiagen). DNA concentration and purity were evaluated and measured spectrophotometrically by reading the absorbance at 260 and 280 nm using the NanoDrop ND 1000 (NanoDrop Technologies).

Transmission electron microscopic (TEM) investigations

In order to perform transmission electron microscopic investigations, small tissue fragments about 2–3 mm^3 from seven mammary tumors resulted by surgery as curative therapy from the patients suffering from mammary carcinoma (surgeon obtained consent from all patients) were processed following the routine TEM protocol [16]. Semithin sections were stained with 1% toluidine blue for light microscopy. Ultrathin sections were cut using a diamond knife and collected on 200 mesh grids and double counterstained with uranyl acetate and subsequently lead citrate. The grids were examined by a transmission electron microscope JEOL JEM-1400 operated at an acceleration voltage of 80kV.

High-resolution melting (HRM) assay

Polymerase chain reaction (PCR) amplifications and HRM analysis were performed in a LightCycler 480 real-time PCR system (Roche Romania) with a 96-well plate. PCR assays were carried out in 20 µL reaction volume containing: 30 ng of genomic DNA, 10 µL Master Mix, 2× concentrated, including ResoLight high-resolution melting dye, 3.5 mM $MgCl_2$, 250 nM of each primer, and PCR grade water. Primer pairs for PIK3CA exons 1, 9 and 20 were previously described [17, 18]. The PCR amplification started with a single enzyme activation step at 95^0C for 10 s, followed by a 45 cycle program [denaturation at 95^0C for 10 s, a touchdown of 65^0C to 57^0C (for exons 1 and 20) and, of 65^0C to 59^0C (for exon 9) for 15 s, elongation at 72^0C for 15 s with a single acquisition mode]. The PCR amplification was followed by a melting program consisting of: denaturation at 95^0C for one minute, renaturation at 40^0C for one minute and subsequent melting with continuous fluorescence measurement from 60^0C to 90^0C at the rate of 25 acquisitions/^{0}C. HRM data were analyzed using Gene-Scanning Software *ver.* 1.0 (Roche Romania). Wild type and mutant samples were identified according to the normalized temperature-shifted differential plot. All samples were tested in duplicate and control samples of MCF7, T47D and SKBR3 DNA were included in each HRM run. The sensitivity test was performed by diluting mutated DNA with wild-type DNA in order to obtain a mutant to wild-type allelic ratio of 25%, 12.5%, 6.2%, 3.1% and 1.5%, respectively.

DNA sequencing

To confirm HRM assay results, all identified samples were subjected to direct bidirectional Sanger sequence analysis. Each sample was amplified using M13-tagged primers. PCR primer pairs (5'-tgtaaaacgacggccagtGGG AAAATGACAAAGAACAGC-3' and 5'-caggaaacagctat gaccTCCATTTTAGCACTTACCTGTGAC-3') and (5'-tgtaaaacgacggccagtCTGAGCAAGAGGCTTTGGAG-3' and 5'-caggaaacagctatgaccCCTATGCAATCGGTCTTT GC-3') with M13 tails (lower case letters) were used respectively to amplify exons 9 and 20 of the *KRAS* gene. The length of the amplicons, including the M13 tails, is of 166 bp and 238 bp, respectively.

PCR was performed in a 25 µL reaction volume containing: 50 ng of genomic DNA, 200 nM forward and 200 nM reverse primers; 0.2 mM dNTPs (each); 2.0 mM $MgCl_2$; 1× PCR buffer; and 1.0 U HotStarTaq DNA polymerase (Qiagen). Reactions were cycled on a Eppendorf Mastercycler Gradient under the following conditions: one cycle at 96^0C for 15 minutes; 30 cycles at 94^0C for 30 s, 58^0C for 30 s, and 72^0C for 45 s; and a final extension step at 72^0C for 10 minutes. Amplified products were visualized on a 2% agarose gel. In order to remove unincorporated primers and dNTPs, 5 µL of PCR products were treated with 2 µL ExoSAP-IT enzyme (USB Corporation, Cleveland, OH, USA) according to manufacturer's instructions.

For sequencing reaction, 1 µL of purified PCR amplification products were used with 4.0 µL BigDye Terminator v3.1 Cycle Sequencing Kit (Applied Biosystems) and 3.2 pmol/µL M13 forward or reverse

primer, in a 10 μL final volume. Cycle sequencing was performed on a Veriti 96-well Thermal Cycler (Applied Biosystems) under the following conditions: heat activation at 96^0C for one minute followed by 25 cycles of 96^0C for 10 s, 50^0C for 5 s and 60^0C for 2 minute. Cycle Sequencing reactions were cleaned up using BigDye Terminator purification kit (Applied Biosystems). Purified sequencing products were resolved by capillary electrophoresis on an Applied Biosystems 3500 Genetic Analyzer with POP-7 polymer and a 50 cm array length. Sequences were aligned to a reference sequence using Variant Reporter Software v1.1 (Applied Biosystems).

Results

Ultrastructural analysis

In case of normal human breast, the mammary tissue is represented by (1) epithelia organized as ducts, ductules and lobules and (2) stroma represented by connective tissue (mostly fibroblasts), including adipose tissue as mammary fat pad. Histological examination of normal human mammary gland shows that mammary ducts and ductules are composed of epithelial arranged in one single uninterrupted layer facing a lumen, which by their basal pole become in contact with myoepithelial cells or direct with the basal lamina. The apical pole of epithelial cells facing the lumen exhibits microvilli. Near the lumen, adjacent epithelial cells exhibit reminiscent of junctional complexes. Desmosomal junctions are irregularly distributed. Ultrastructurally, the nuclei of epithelial cells have a regular shape (contour). Their chromatin is evenly distributed. Normal as size and infrastructure, nucleoli are embedded in nuclear chromatin.

Inside of normal epithelial cell cytoplasm, few profiles of rough endoplasmic reticulum, few mitochondria, scattered free ribosomes and rare dictiosomal elements of Golgi apparatus can be seen. Concerning the cytoskeleton, fine filaments are perinuclear distributed or reach the inner plaque of desmosomal junctions. Sometimes, vacuoles of different size and osmiophilic vesicles can be seen. Moreover, pinocytotic vesicles can be detected along the plasma membrane facing the basal lamina and intercellular spaces.

The above-described general picture concerning normal histoarhitecture of the human mammary gland was dramatically changed when the tumoral mammary tissue were electron microscopic investigated. Neoplastic cells exhibit a high nucleus/cytoplasm ratio. Euchromatin is predominantly; heterochromatin is mostly attached to the inner membrane of the nuclear envelope (Figure 1). Desmosomal junctions are rare, almost missing, but interdigitating junctions are detectable. Some desmosomes are internalized (Figure 2). Often, intracellular lumens exhibiting microvilli can be seen (Figure 3). Some nuclei have large nucleoli. As many desmosomes are impaired, remnants of a desmosomal plaque can be detected (Figure 4). Moreover, for long profile at the presumptive cell–cell contact between the tumor cells, no specialized cell–cell junction can be detected. Particularly, very long white crystalline rod can be seen near the nucleus of a tumor cell. Three centriols can be counted inside the cytoplasm (Figure 5). Tumor invadopodia penetrate deeply inside of the peritumoral stroma. Shedding membrane vesicles produced by tumor cells can be delivered into tumor stroma (Figures 6 and 7). Endothelial wall of the blood microvasculature represented by endothelial cells exhibiting prominent nuclei towards the capillary lumen are interconnected by tight junctions. Often, pericytes are missing. Apart from the usual basement membrane around the endothelial wall, redundant basement membranes and a lot of amorphous material can be seen (Figure 8). Sometimes, fenestrated blood vessel can be detected inside of the mammary carcinoma tumor (Figure 9). When present, pericytes appear to be partial detached from the endothelial wall by redundant basement membranes and the excessive amorphous material. Mention must be made that telocytes can be detected in close vicinity of blood capillaries but not in direct contact with endothelial cells or pericytes (Figure 10). Interestingly, invadopodial tumor cell extension may penetrate deeply inside of peritumoral stroma and dissociate the pericyte from the endothelial wall (Figure 11).

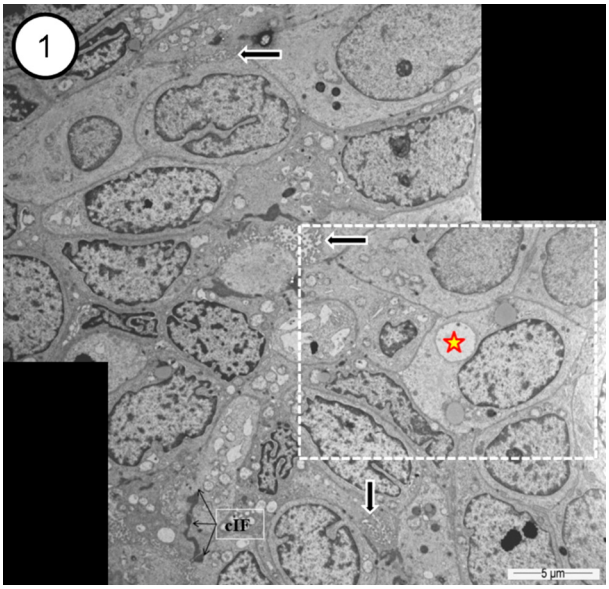

Figure 1 – ***An overview from a large area of mammary tumor carcinoma. Almost all tumor cells have a high nucleus/cytoplasm ratio. Euchromatin is predominant while heterochromatin is mostly attached to the inner membrane of the nuclear envelope. Two small lumens are visible (arrows). A red star marks a presumable intracellular lumen. Conglomerates of intermedium filaments (cIF) can be seen.***

Molecular investigations

Serial dilutions of MCF7 or T47D genomic DNA in wild-type SKBR3 DNA were prepared in order to asses HRM sensitivity. The technique allowed the detection of 3% and 6% of cell line DNA known to harbor PIK3CA E545K and H1047R mutations, respectively (Figure 12). Aberrant melt profiles were observed in 10 (47.6%) breast tumor samples. Three of them suggested the presence of mutations in exon 9 (14.3%), and seven in exon 20 (33.3%) of the PIK3CA gene. In PIK3CA exon 1, mutations have not been detected. Eleven tumor samples were found to contain wild-type DNA (52.4%). No difference in the melt profiles was observed in normal tissue sample pairs comparing with wild-type control (Figure 13). Parallel testing by Sanger sequencing confirmed only eight of 10 samples determined to be positive by the HRM assay. For the exons 9 and 20 of the PIK3CA gene, three variants we identified, E545K, Q546K, and H1047R (Figure 14).

Somatic mutations E545K and Q546K, located within helical domain, accounted for 12.5% mutations each, meanwhile H1047R mutation within kinase domain was detected in 75.0% of mutant tumor samples.

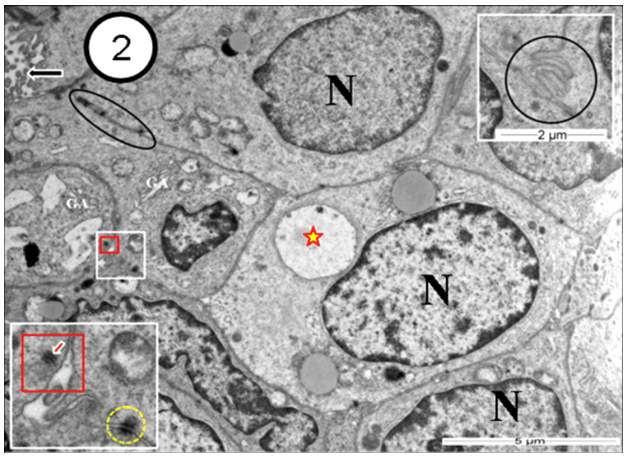

Figure 2 – ***Few tumor cells with polymorphic and large nuclei (N) are tightly apposed each other. Desmosomal junctions are rare (elliptic area and yellow dotted circle in the left down inset), almost missing, but interdigitating junctions (encircled areas in the upper right inset) are detectable. An internalized desmosome in red square, detailed in the left down inset (arrow) is detectable. GA: Golgi apparatus.***

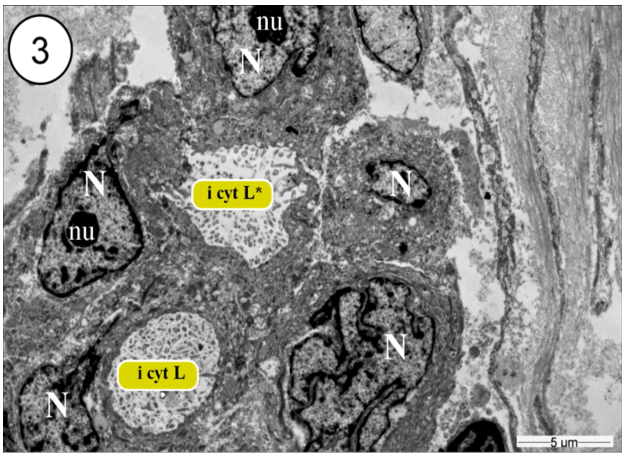

Figure 3 – ***Hyperplastic mammary tissue represented by neoplasic cells exhibits a high N/C ratio. Nuclei (N) are prevalently occupied by euchromatin. Some nuclei have large nucleoli (nu). Intracellular lumens (i cyt L) exhibit microvilli; one of them (i cyt L*) communicates with the extracellular space.***

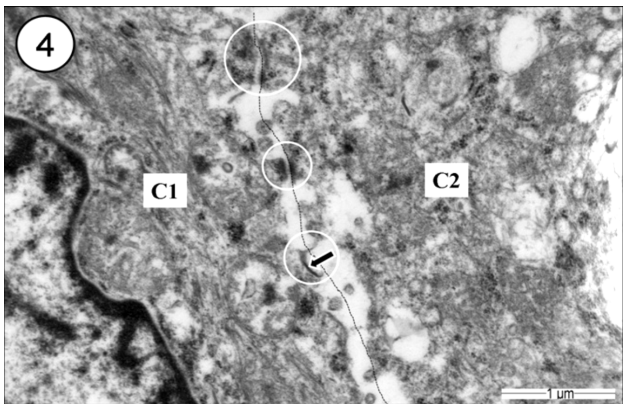

Figure 4 – ***Between two tumor cells C1 and C2 (dotted line), there are impaired desmosomes (encircled areas). Arrow marks a remnant of a desmosomal plaque.***

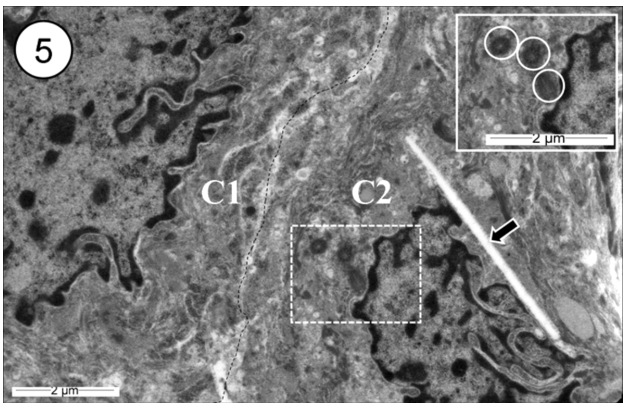

Figure 5 – ***At the presumptive cell–cell contact (dashed line) between the tumor cells (C1) and (C2), no specialized cell–cell junction can be detected. A very long white crystalline rod (arrow) can be seen near the nucleus (N). Inset: Three centriols (encircled areas) can be counted inside the cytoplasm.***

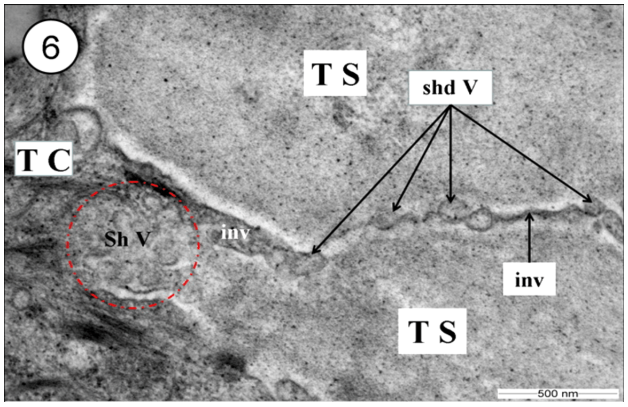

Figure 6 – ***Inside of the peritumoral stroma (TS), a terminal-end of a tumor invadopodium (inv) with shedding membrane vesicles (shd V) is visible. Shedding membrane vesicles (Sh V) produced by tumor cell (TC) are in way to be delivered into tumor stroma (TS).***

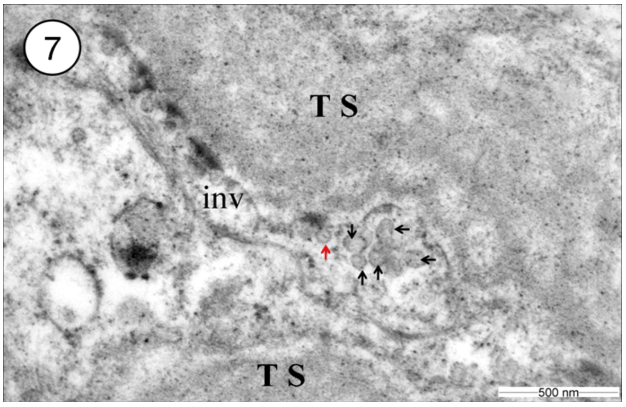

Figure 7 – ***A very thin invadopodia (inv) originated from a tumor cell deeply penetrates inside of the tumor stroma (TS). Shedding membrane vesicles (black arrows) are detectable; one of them (red arrow) is attached to the plasma membrane.***

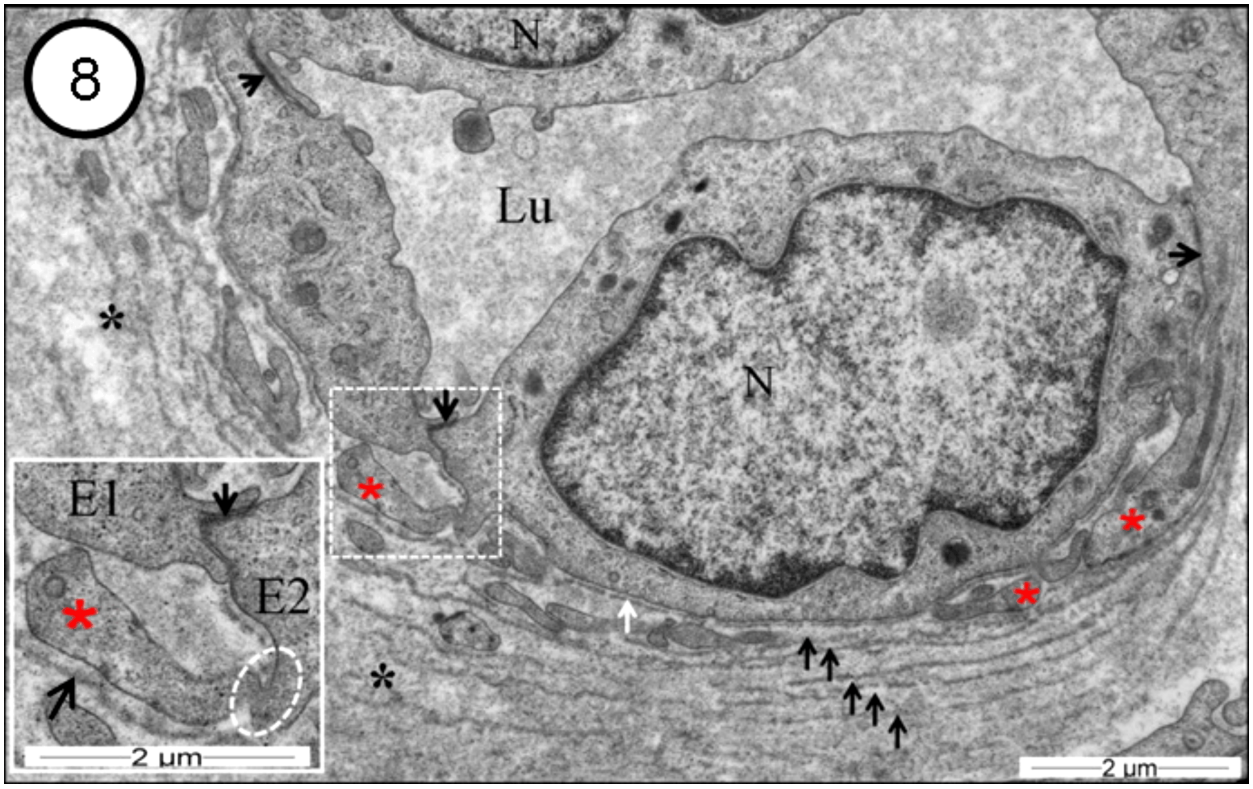

Figure 8 – ***Blood vessel inside of the mammary carcinoma showing endothelial cells with prominent nuclei (N) interconnected by tight junctions (head arrow). Apart from the usual basement membrane around the endothelial wall (white arrow), few other redundant basement membranes (black arrows) and a lot of amorphous material (asterisks) can be seen. Lu: Lumen. In inset: A small protrusion (red asterisk) belongs to an endothelial cell (elliptic area). An interendothelial junction (head arrow) between two endothelial cells (E1 and E2) can be seen. Arrow marks a patch of basement membrane.***

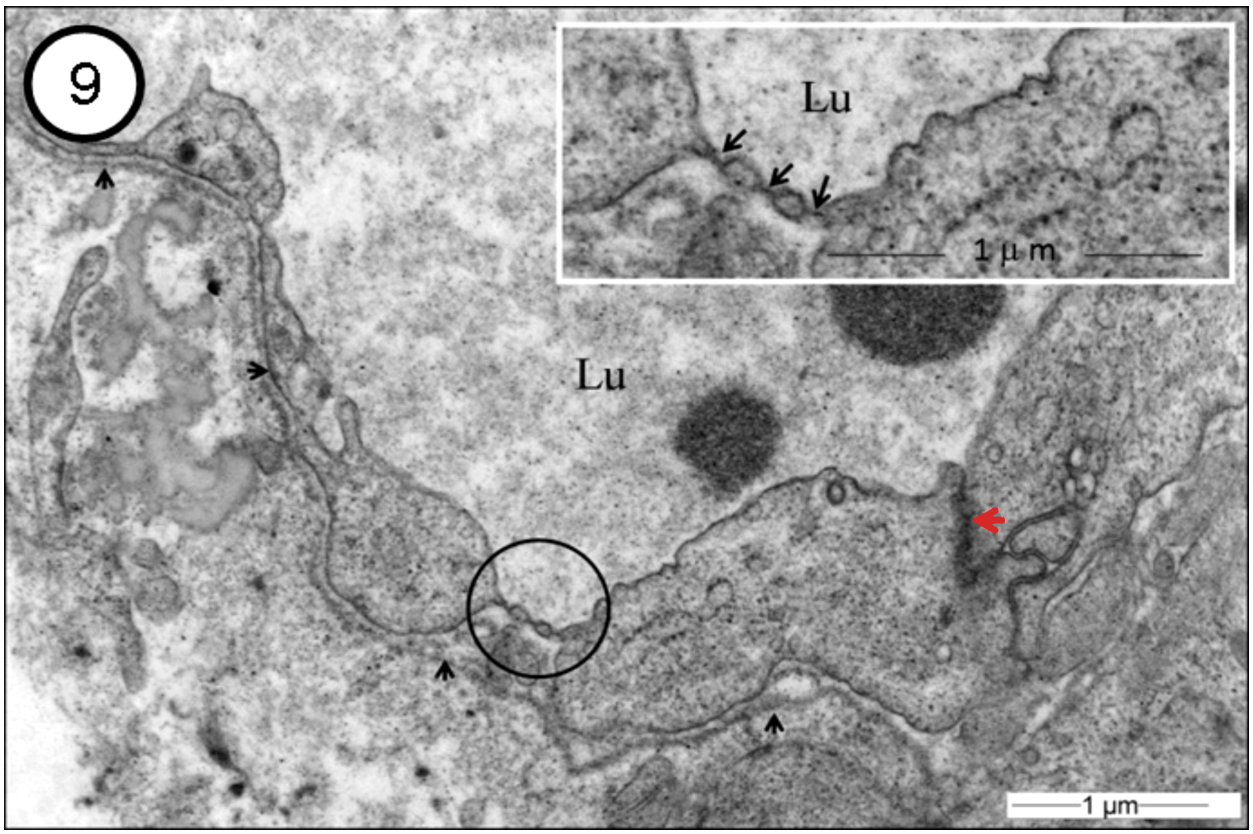

Figure 9 – ***A sector of a blood fenestrated vessel (encircled area) located inside of the mammary carcinoma tumor. A continuous basement membrane (head arrows) follows endothelial wall. Lu: Lumen. In inset: A high magnification of the capillary fenestration (arrows). Lu: Lumen.***

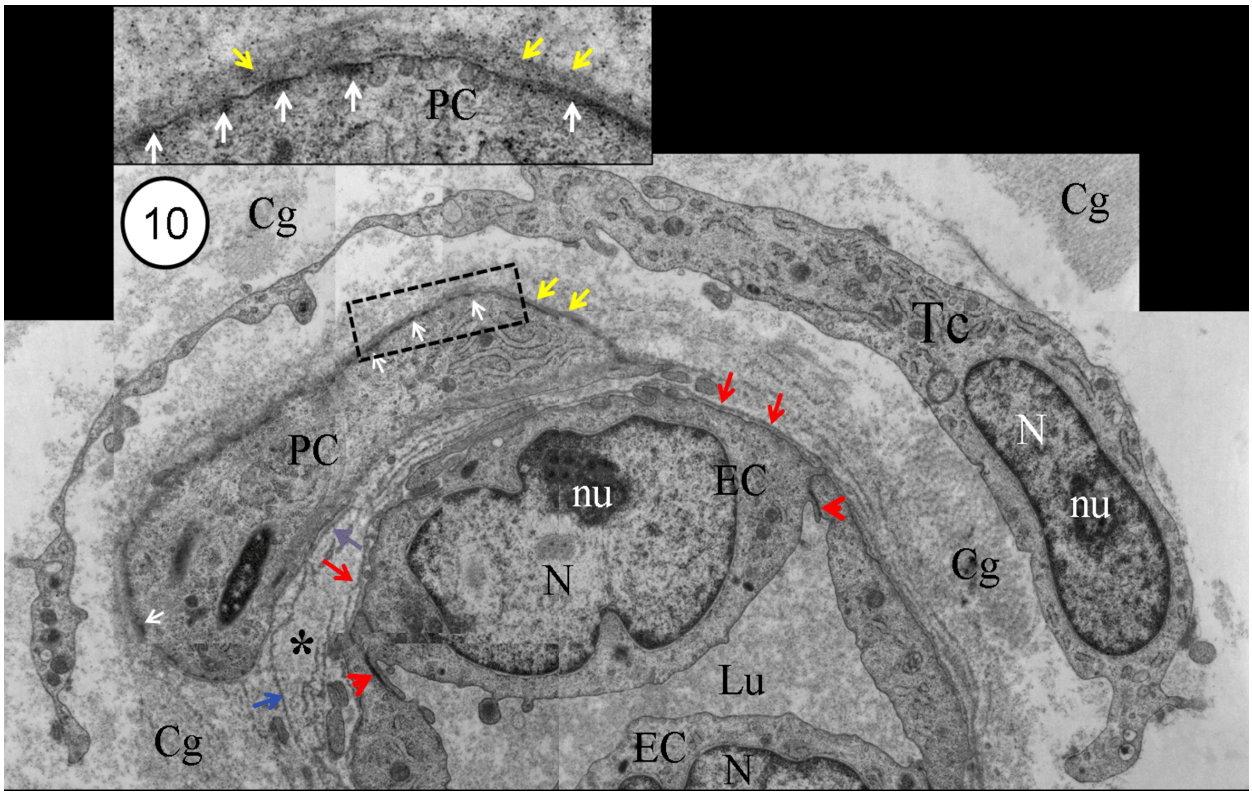

Figure 10 – ***Endothelial cells (EC) have prominent nuclei (N). A pericyte (PC) appears to be partial detached from the endothelial wall by redundant basement membranes (red, pink and blue arrows) and an excessive amorphous material (asterisk). Characteristic subplasmalemal dense plaques of the inner face of external pericytic plasma membrane (white arrows) can be detected (see the detail in inset, where yellow arrows mark the basement membrane associated to the pericyte). A telocyte (Tc) can be detected in close vicinity of the blood capillary but not in direct contact with endothelial cells or the pericyte. N: Nuclei; nu: Nucleoli; Lu: Lumen. Inter-endothelial junctions (head arrows). Cg: Collagen.***

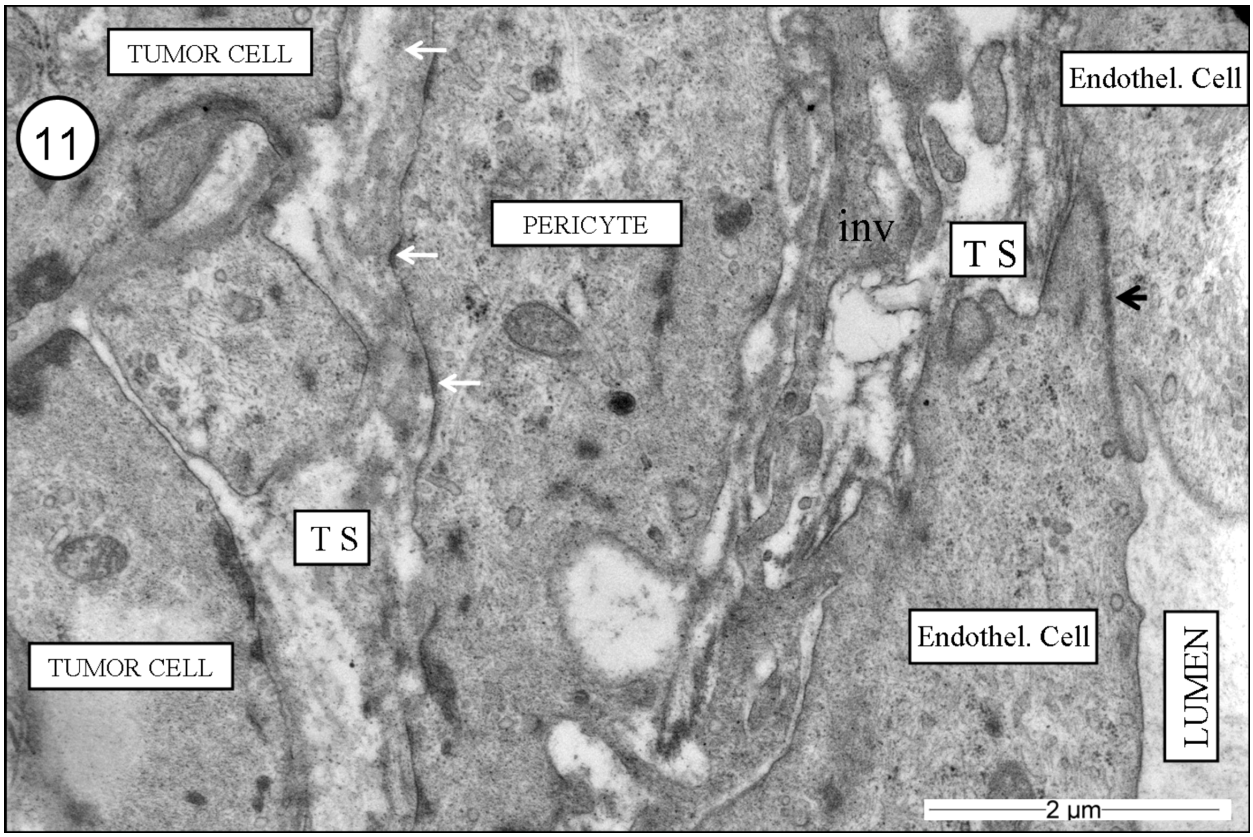

Figure 11 – ***An invadopodia (inv) belonging to a tumor cell penetrates deeply inside of peritumoral stroma (TS) and dissociate the pericyte from the endothelial wall. Head arrow marks the tight junction between two endothelial cells. White arrows mark characteristic subplasmalemmal dense plaques of the pericyte.***

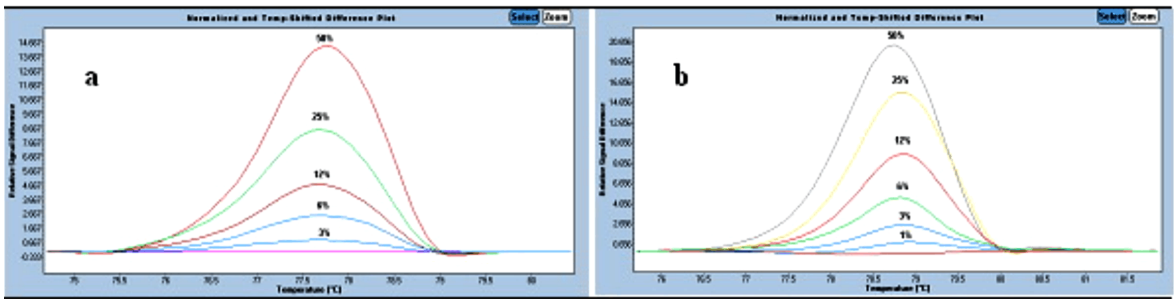

Figure 12 – ***Sensitivity curves for exon 9 (a) and exon 20 (b), respectively.***

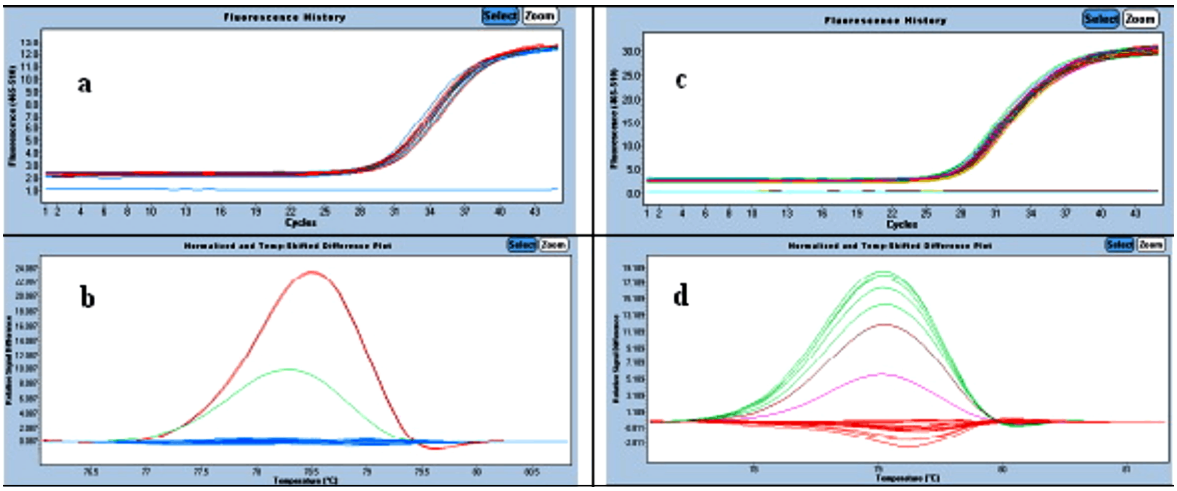

Figure 13 – ***Amplification (a) and dissociation (b) curves for exon 9; amplification (c) and dissociation (d) curves for exon 20 of the PIK3CA gene. All amplification curves produced a crossing point of <30 and reached a similar plateau height.***

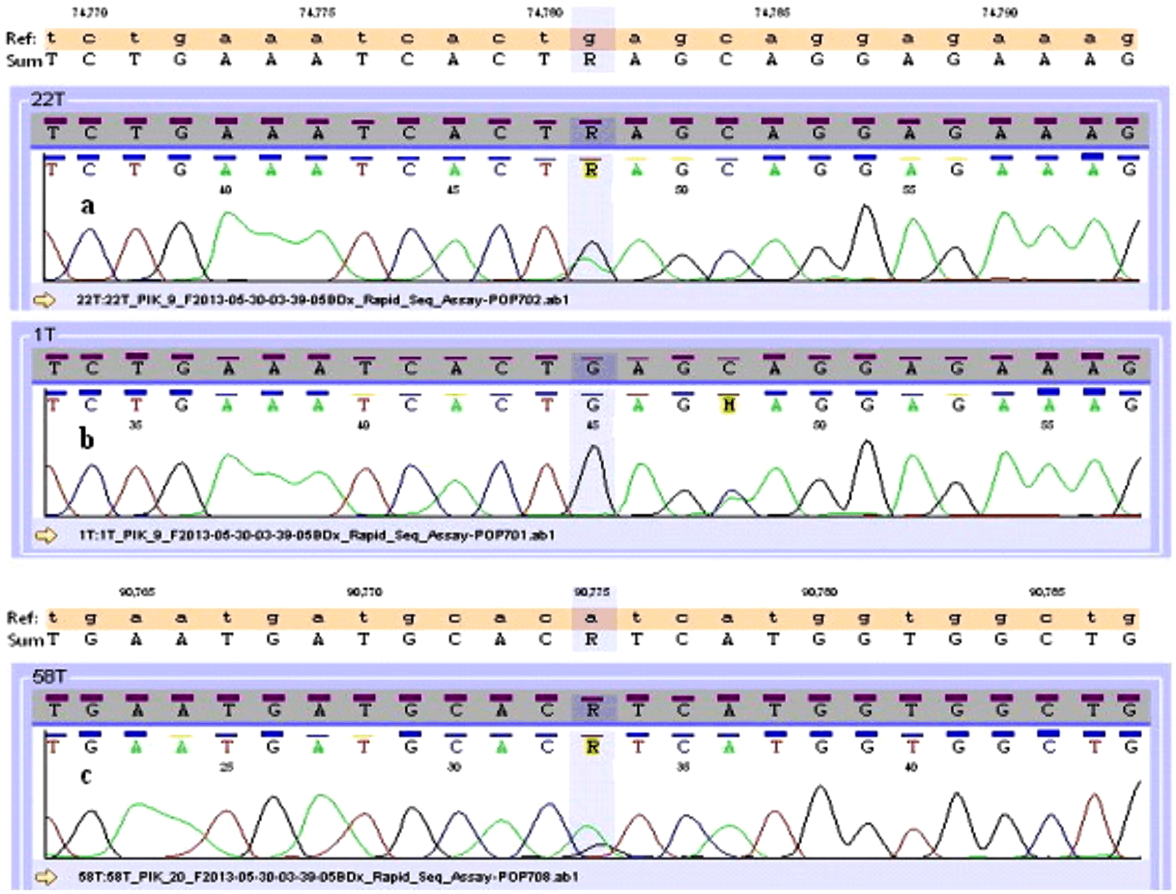

Figure 14 – ***Electroferograms for mutation identified (a) E545[K,E], G>A; (b) Q546[K,Q], G>A; (c) H1047[H,R], A>G.***

Discussion

Ultrastructural aspect of tumor cells

Almost human cancers have an epithelial origin. In breast cancer, glandular epithelium as well as myoepithelial cells can be involved.

Inside of TEM investigated invasive mammary carcinoma tumor, neoplastic cells represented by glandular epithelium exhibit a high nucleus/cytoplasm ratio. Nuclei are polymorphic. Moreover, atypical mitosis is quite frequently. Euchromatin is predominantly; heterochromatin is mostly attached to the inner membrane of the nuclear envelope (Figures 1–3). This is a general aspect of the nucleoplasm in case of tumor cells. On consider that nuclear organization itself can modulate cellular and tissue phenotype. While heterochromatin remains transcriptionally silent, euchromatin is considered more easily transcribed [2, 19–21].

Intracellular lumens with microvilli are frequently encountered (Figure 3). Intracellular lumens containing microvilli have been described previously, especially, but not exclusively, in invasive carcinomas [2].

Cell–cell and cell–extracellular matrix relationships

Internalization of desmosomes

Normal epithelial cells of mammary gland are polarized cells. In order to maintain their polarized status, epithelial cells must keep relative stable cell–cell and cell–extracellular matrix relationships. For that, specialized cell junctions are developed and must be conserved unaltered in their infrastructure and molecular composition. Indeed, to maintain 3-D histoarchitecture and communication between neighboring cells in epithelia, cell–cell and cell–extracellular matrix specialized junctional adhesion structures must be well developed and preserved. Cell–cell cohesion is maintained by junctional complex, mainly represented by desmosomes. By anchoring desmosomal cadherins of adjacent cells to the intermediate filaments cytoskeleton, desmosomal junctions contribute to the histo-architecture organization and maintenance [22, 23]. Examination by transmission electron microscopy and immune electron microscopy of desmosome revealed that specific infrastructures and molecular components are very precisely located as extracellular, transplasmalemmal and intracellular domains [2, 24]. Desmosome integrity depends on the tightly regulatory mechanisms. Alteration of the junctional adhesions may involve more or less tissue disorganization and consequently disfunctionalities (just to mention cell depolarization or cell migration). In a case of mammary carcinoma, we had investigated internalization of some desmosomes can be detected as is depicted in Figure 2. Because many desmosomes are impaired or are totally missing, quite often some tumor cells lost completely their contacts with the other neighboring tumor cells. Displacement/disorganization of desmosomes may follow different ways. One of that is internalization of desmosomes. It occurs when Ca^{2+} level is under normal level [25]. Burdett [26] demonstrated that internalization of desmosomes and their entry into endocytotic pathway *via* late endosomes in MDCK cells may also occur at the normal Ca^{2+} level. Kimura *et al*. [22] reported that loss of calcium independence involves an "inside-out" transmembrane signal generated by protein kinase C (PKC).

Tumor–stroma interactions in breast cancer

A solid tumor is a very sophisticated system, mostly represented by (1) permanent genetic altered cells and associated tumor stroma represented by resident or transiently cells (fibroblasts, fibrocytes, endothelial cells and pericytes of the capillary, telocytes, inflammatory cells, naked or mielinated nerves, myoepithelial cells, etc.) as well as extracellular matrix represented by identifiable infrastructures (basement membrane, collagen or elastic fibers, exosomes, etc.) or soluble molecules (cytokines, hormones, growth factors, etc.). In order to maintain their viability and to grow uncontrolled, tumor cells need autocrine and paracrine support [19, 21].

Very often, the basement membrane is missing at the tumor–stroma interface. It is well documented that basement membrane integrity is a prerequisite for epithelia morphogenesis during embryo development. BM regulates epithelial–mesenchymal interactions [2]. Epithelial cells facing basement membrane maintain their morpho-functional phenotype of polarized cell as long as the adjacent basement membrane remains unaltered in their molecular composition. Any mutation in their components and infrastructural alterations of basement membrane lead to wide variety of clinical phenotypes (specific diseases), including invasive cell growth in case of cancer [27, 28].

Shedding membrane vesicles

Some tumor cells from invasive mammary carcinoma produce and shed membrane vesicles. Such kind of infrastructures can be detected either close to the body cell or delivered by invadopodia (Figures 6 and 7). Extracellular vesicles are nano-membranous infrastructures ranging from 30–2000 nm in diameter that are released from many cell types into the extracellular microenvironment. Mention must be made that nomenclature, biogenesis and their roles are still a matter of debate [29]. Extracellular vesicles, especially exosomes contain diverse small molecules as proteins, lipids, microRNAs, mRNA and DNA fragments, which act as mediators of intercellular communications by inducing phenotypic changes in recipient cells [29, 30]. Telocytes also may contribute to extracellular vesicles deliverance [21, 31, 32].

Tumor stroma microvasculature status

Concerning microvasculature status of investigated invasive mammary carcinoma, mention must be made that in almost cases, the mainly abnormalities we observed are restricted to the fenestration of blood capillary and displacements of the pericytes, either by redundant basement membranes, amorphous material or infiltration of tumor cell invadopodia between pericytes and endocytes (as is depicted in Figures 8, 9 and 11). A mature and stable blood capillary requires a presence of a special cell phenotype, namely pericyte, around the abluminal face of the vessel tube [33]. Endothelial wall fenestrations and pericytes displacement or totally absence of pericytes were also observed in skin basal and squamous cell carcinoma were also reported [21, 34, 35].

Telocytes inside of the tumor stroma

Nowadays is well documented that mammary stroma play a major role in the breast homeostasis. Moreover, a body of evidence suggests that genetic mutations can and do occur initially inside of breast stroma, so that stroma itself become an oncogenic agent and can induce and sustain tumorigenicity in adjacent cells [36]. Among the well-known resident cell types as tumor-stroma components, just to mention fibroblasts, myofibroblasts, endothelial cells, nerves, a new identified cell phenotype termed telocyte got a remarkable attention [21, 31, 37]. Telocytes were described as interstitial cells in very different normal tissues: [31, 37–39]. By their homo- and hetero-cellular junctions telocytes may participate in intercellular signaling [40], able to modulate tissues homeostasis similar to a very primitive nervous system at the cellular level [41]. Telocytes seem to be involved in many physiological and pathological processes [42]. In all mammary carcinoma cases we analyzed in the present study, telocytes of the tumor stroma often are identified in the close vicinity of some other interstitial cells types (not shown), but rather missing the direct contact, as is depicted in Figure 10. In a recent published paper, we reported that in basal cell carcinoma and squamous cell carcinoma both cutaneous cancer, telocytes have a very restraint number of hetero-cellular junctions [21].

Genetic analysis

Genetic and biochemical evidence has been brought forward to demonstrate that activation of PI3K/AKT pathway contributes to the appearance and development of breast cancer [3, 9]. PIK3CA is one of the key molecules involved in PI3K/AKT signaling. Activating somatic mutations in PIK3CA gene result in enhanced downstream signaling and oncogenic transformation in vitro. Hot-spot mutations in kinase and helical domains are thought to be early events in breast cancer.

The prognostic value of PIK3CA mutations in breast cancer remains questionable. In a recent study that included 2587 breast tumor specimens from 12 independents studies [43], was found a favorable clinical response in a subgroup of postmenopausal women with ER positive breast cancer and mutations in kinase domain of p110α. Regarding the relative prognostic value of PIK3CA mutations in each exon in part also remains a questionable problem. Some researchers have found that mutations in exon 9 have a poorer prognosis than mutation in exon 20 [44], while other researchers have concluded that the mutations in the PIK3CA exon 20 would actually those with poor prognosis [45, 46]. Regarding to metastasis-free survival there is no difference between patients with mutations in exon 9 compared with those with mutations in exon 20 [47].

In this study, we used HRM assay and direct DNA sequencing to look for mutations in exons 1, 9 and 20 of PIK3CA gene in 21 breast cancer patients. HRM assay provides a cost-efficient, simple and rapid approach to successfully screening tumor samples for somatic mutations. The assay used in our study showed a capability to detect as low as 3% and 6% of mutant DNA in the presence of wild-type DNA for PIK3CA exons 9 and 20. Using HRM assay we were able to detect mutations in exons 9 and 20 of the PIK3CA gene in 10 of the total 21 tumor samples. No mutations were found in normal tissue pairs.

Of the 21 sample pairs analyzed by two methods, concordance was of 95.0%. One mutation in exon 9 and one in exon 20 could not be confirmed by Sanger sequencing. Two somatic variants were detected by direct sequencing in exon 9 (E545K and Q546K), and one in exon 20 (H1047R). E545K and H1047R are hot spot mutations with a reported frequency of 20% and 55% respectively. Q546K is a rare, cancer-specific mutation that accounts for less than 1% of total PIK3CA mutations in breast cancers. Functional studies suggested that these particular *PIK3CA* mutations lead to increased PI3K activity and induce oncogenic transformation *in vitro*. The discrepancy may be explained by reduced sensitivity of DNA direct sequencing in samples with less than 30% tumor content. Significant number bioptic tumor tissues are characterized by genotypic and cell heterogeneity. A low content of mutant cells can lead to falls-negative results in Sanger sequencing. Tumor enrichment by laser microdissection and selection of a highly sensitive method employed for mutations detection could partially addressed this problem. In accord with studies previously published, our results showed that HRM assay is more accurate in mutations detection comparing with Sanger sequencing.

Conclusions

Electron microscopy investigations revealed that in invasive mammary carcinoma intercellular junctions, namely desmosomes are severely altered. Tumor cells generate and disseminate membrane vesicles, including exosomes inside of peritumoral stroma. Hetero-cellular contacts of telocytes were reduced, which suggest a possible perturbation of tissue homeostasia modulation. Our study confirms the high prevalence of PIK3CA mutations in breast cancer. In accordance with the results of the largest previous studies, 87.5% of mutations detected by DNA direct sequencing were hot spot mutations, most of them located in the kinase domain. High percentage of mutations detected by HRM makes the assay an attractive choice for mutation scanning, especially in samples with low percentage of tumor cell.

Conflict of interests

The authors declare that they have no conflict of interests.

Acknowledgments

The authors acknowledge for financing support done to perform and to write the paper coming from: Project No. RO1567-IBB07/2012 from the Institute of Biology Bucharest of Romanian Academy and Project Parteneriate No. 4/2012 from the Executive Agency for Higher Education, Research, Development and Innovation Funding, Bucharest, Romania. Corina Elena Mihalcea is PhD student by Doctoral programme at the SCOSAR of Romanian Academy. Ana-Maria Moroşanu and Daniela Murărașu are PhD students at the Romanian Academy. Electron microscopic investigations were performed by a transmission electron microscope JEOL JEM 1400, supported by DIBIOCLIM Project. The authors thank A. Brînzan and V. Stan for technical assistance.

References

[1] Yang M, Chen J, Su F, Yu B, Su F, Lin L, Liu Y, Huang JD, Song E. Microvesicles secreted by macrophages shuttle invasion-potentiating microRNAs into breast cancer cells. Mol Cancer, 2011, 10:117.

[2] Mirancea N, Mirancea D. Ultrastructura celulelor şi ţesuturilor. Ed. Ars Docendi, Universitatea din Bucureşti, 2010.

[3] Stemke-Hale K, Gonzalez-Angulo AM, Lluch A, Neve RM, Kuo WL, Davies M, Carey M, Hu Z, Guan Y, Sahin A, Symmans WF, Pusztai L, Nolden LK, Horlings H, Berns K, Hung MC, van de Vijver MJ, Valero V, Gray JW, Bernards R, Mills GB, Hennessy BT. An integrative genomic and proteomic analysis of PIK3CA, PTEN, and AKT mutations in breast cancer. Cancer Res, 2008, 68(15):6084–6091.

[4] Samuels Y, Waldman T. Oncogenic mutations of PIK3CA in human cancers. Curr Top Microbiol Immunol, 2010, 347:21–41.

[5] Dupont Jensen J, Laenkholm AV, Knoop A, Ewertz M, Bandaru R, Liu W, Hackl W, Barrett JC, Gardner H. PIK3CA mutations may be discordant between primary and corresponding metastatic disease in breast cancer. Clin Cancer Res, 2011, 17(4):667–677.

[6] Liedtke C, Cardone L, Tordai A, Yan K, Gomez HL, Figureoa LJ, Hubbard RE, Valero V, Souchon EA, Symmans WF, Hortobagyi GN, Bardelli A, Pusztai L. PIK3CA-activating mutations and chemotherapy sensitivity in stage II–III breast cancer. Breast Cancer Res, 2008, 10(2):R27.

[7] Chalhoub N, Baker SJ. PTEN and the PI3-kinase pathway in cancer. Annu Rev Pathol, 2009, 4:127–150.

[8] Castaneda CA, Cortes-Funes H, Gomez HL, Ciruelos EM. The phosphatidyl inositol 3-kinase/AK signaling pathway in breast cancer. Cancer Metastasis Rev, 2010, 29(4):751–759.

[9] Saal LH, Holm K, Maurer M, Memeo L, Su T, Wang X, Yu JS, Malmström PO, Mansukhani M, Enoksson J, Hibshoosh H, Borg A, Parsons R. PIK3CA mutations correlate with hormone receptors, node metastasis, and ERBB2, and are mutually exclusive with PTEN loss in human breast carcinoma. Cancer Res, 2005, 65(7):2554–2559.

[10] Berns K, Horlings HM, Hennessy BT, Madiredjo M, Hijmans EM, Beelen K, Linn SC, Gonzalez-Angulo AM, Stemke-Hale K, Hauptmann M, Beijersbergen RL, Mills GB, van de Vijver MJ, Bernards R. A functional genetic approach identifies the PI3K pathway as a major determinant of trastuzumab resistance in breast cancer. Cancer Cell, 2007, 12(4):395–402.

[11] Nagata Y, Lan KH, Zhou X, Tan M, Esteva FJ, Sahin AA, Klos KS, Li P, Monia BP, Nguyen NT, Hortobagyi GN, Hung MC, Yu D. PTEN activation contributes to tumor inhibition by trastuzumab, and loss of PTEN predicts trastuzumab resistance in patients. Cancer Cell, 2004, 6(2):117–127.

[12] Wong KK, Engelman JA, Cantley LC. Targeting the PI3K signaling pathway in cancer. Curr Opin Genet Dev, 2010, 20(1):87–90.

[13] Martinez-Martí A, Felip E. PIK3 pathway in NSCLC. Front Oncol, 2012, 1:55.

[14] Engelman JA, Luo J, Cantley LC. The evolution of phosphatidylinositol 3-kinases as regulators of growth and metabolism. Nat Rev Genet, 2006, 7(8):606–619.

[15] Miller TW, Rexer BN, Garrett JT, Arteaga CL. Mutations in the phosphatidylinositol 3-kinase pathway: role in tumor progression and therapeutic implications in breast cancer. Breast Cancer Res, 2011, 13(6):224.

[16] Mirancea N, Hausser I, Metze D, Stark HJ, Boukamp P, Breitkreutz D. Junctional basement membrane anomalies of skin and mucosa in lipoid proteinosis (hyalinosis cutis et mucosae). J Dermatol Sci, 2007, 45(3):175–185.

[17] Fadhil W, Ibrahem S, Seth R, Ilyas M. Quick-multiplex-consensus (QMC)-PCR followed by high-resolution melting: a simple and robust method for mutation detection in formalin-fixed paraffin-embedded tissue. J Clin Pathol, 2010, 63(2): 134–140.

[18] Simi L, Pratesi N, Vignoli M, Sestini R, Cianchi F, Valanzano R, Nobili S, Mini E, Pazzagli M, Orlando C. High-resolution melting analysis for rapid detection of KRAS, BRAF, and PIK3CA gene mutations in colorectal cancer. Am J Clin Pathol, 2008, 130(2):247–253.

[19] Bissell MJ, Weaver VM, Lelièvre SA, Wang F, Petersen OW, Schmeichel KL. Tissue structure, nuclear organization, and gene expression in normal and malignant breast. Cancer Res, 1999, 59(7 Suppl):1757s–1763s; discussion 1763s–1764s.

[20] Tamaru H. Confining euchromatin/heterochromatin territory: jumonji crosses the line. Genes Dev, 2010, 24(14):1465–1478.

[21] Mirancea N, Moroşanu AM, Mirancea GV, Juravle FD, Mănoiu VS. Infrastructure of the telocytes from tumor stroma in the skin basal and squamous cell carcinomas. Rom J Morphol Embryol, 2013, 54(4):1025–1037.

[22] Kimura TE, Merritt AJ, Garrod DR. Calcium-independent desmosomes of keratinocytes are hyper-adhesive. J Invest Dermatol, 2007, 127(4):775–781.

[23] Stahley SN, Saito M, Faundez V, Koval M, Mattheyses AL, Kowalczyk AP. Desmosome assembly and disassembly are membrane raft-dependent. PLoS One, 2014, 9(1):e87809.

[24] Mirancea N, Mirancea D, Fusenig NE, Breitkreutz D. Immuno-electron microscopic detection of the molecular components of the hemidesmosomal junction. Proc Rom Acad Ser B Chem Life Sci Geosci, 2001, 3(2):123–130.

[25] Mattey DL, Garrod DR. Splitting and internalization of the desmosomes of cultured kidney epithelial cells by reduction in calcium concentration. J Cell Sci, 1986, 85:113–124.

[26] Burdett IDJ. Internalisation of desmosomes and their entry into the endocytotic pathway *via* late endosomes in MDCK cells. Possible mechanisms for the modulation of cell adhesion by desmosomes during development. J Cell Sci, 2003, 106(Pt 4): 1115–1130.

[27] Mueller MM, Fusenig NE. Friends or foes – bipolar effects of the tumor stroma in cancer. Nat Rev Cancer, 2004, 4(11): 839–849.

[28] Mirancea N, Moroşanu AM, Juravle FD, Mirancea GV, Trandaburu I, Mănoiu VS. Relevant infrastructural alterations as premalignant lesions during benign tumors development. Rom J Biol Zool, 2011, 56(1):95–112.

[29] Ji H, Chen M, Greening DW, He W, Rai A, Zhang W, Simpson RJ. Deep sequencing of RNA from three different extracellular vesicle (EV) subtypes released from the human LIM1863 colon cell line uncovers distinct miRNA-enrichment signatures. PLoS One, 2014, 9(10):e110314.

[30] Dutta S, Warshall C, Bandyopadhyay C, Dutta D, Chandran B. Interactions between exosomes from breast cancer cells and primary mammary epithelial cells leads to generation of reactive oxygen species which induce DNA damage response, stabilization of p53 and autophagy in epithelial cells. PLoS One, 2014, 9(5):e97580.

[31] Cretoiu SM, Popescu LM. Telocytes revisited. Biomol Concepts, 2014, 5(5):353–369.

[32] Fertig ET, Gherghiceanu M, Popescu LM. Extracellular vesicles release by cardiac telocytes: electron microscopy and electron tomography. J Cell Mol Med, 2014, 18(10):1938–1943.

[33] Stratman AN, Davis GE. Endothelial cell-pericyte interactions stimulate basement membrane matrix assembly: influence on vascular tube remodeling, maturation, and stabilization. Microsc Microanal, 2012, 18(1):68–80.

[34] Mirancea N, Mirancea D, Juravle FD, Şerban AM, Mirancea GV. Epithelial–stromal interactions during tumorigenesis and invasion process of basocellular and squamous cell carcinomas at the tumor–peritumoral stroma interface. Rom J Biol Zool, 2009, 54(1):97–120.

[35] Mirancea N, Mirancea GV, Moroşanu AM, Juravle FD, Mirancea D. Infrastructural and molecular tumor–extracellular matrix interface alterations in the basocellular and squamous cell carcinoma development. Rom J Biol Zool, 2010, 55(1): 95–109.

[36] Kim JB, Stein R, O'Hare MJ. Tumour–stromal interactions in breast cancer: the role of stroma in tumourigenesis. Tumour Biol, 2005, 26(4):173–185.

[37] Popescu LM, Gherghiceanu M, Cretoiu D, Radu E. The connective connection: interstitial cells of Cajal (ICC) and ICC-like cells establish synapses with immunoreactive cells. Electron microscope study *in situ*. J Cell Mol Med, 2005, 9(3):714–730.

[38] Zheng M, Sun X, Zhang M, Qian M, Zheng Y, Li M, Cretoiu SM, Chen C, Chen L, Cretoiu D, Popescu LM, Fang H, Wang X. Variations of chromosomes 2 and 3 gene expression profiles among pulmonary telocytes, pneumocytes, airway cells, mesenchymal stem cells and lymphocytes. J Cell Mol Med, 2014, 18(10):2044–2060.

[39] Rusu MC, Mirancea N, Mănoiu VS, Vâlcu M, Nicolescu MI, Păduraru D. Skin telocytes. Ann Anat, 2012, 194(4):359–367.

[40] Manetti M, Rosa I, Messerini L, Guiducci S, Matucci-Cerinic M, Ibba-Manneschi L. A loss of telocytes accompanies fibrosis of multiple organs in systemic sclerosis. J Cell Mol Med, 2014, 18(2):253–262.
[41] Smythies J, Edelstein L. Telocytes, exosomes, gap junctions and the cytoskeleton: the makings of a primitive nervous system? Front Cell Neurosci, 2014, 7:278.
[42] Bassotti G, Villanacci V, Creţoiu D, Creţoiu SM, Becheanu G. Cellular and molecular basis of chronic constipation: taking the functional/idiopathic label out. World J Gastroenterol, 2013, 19(26):4099–4105.
[43] Dumont AG, Dumont SN, Trent JC. The favorable impact of PIK3CA mutations on survival: an analysis of 2587 patients with breast cancer. Chin J Cancer, 2012, 31(7):327–334.
[44] Lai YL, Mau BL, Cheng WH, Chen HM, Chiu HH, Tzen CY. PIK3CA exon 20 mutation is independently associated with a poor prognosis in breast cancer patients. Ann Surg Oncol, 2008, 15(4):1064–1069.
[45] Cizkova M, Susini A, Vacher S, Cizeron-Clairac G, Andrieu C, Driouch K, Fourme E, Lidereau R, Bièche I. PIK3CA mutation impact on survival in breast cancer patients and in ERα, PR and ERBB2-based subgroup. Breast Cancer Res, 2012, 14(1):R28.
[46] Mangone FR, Bobrovnitchaia IG, Salaomi S, Manuli E, Nagai MA. PIK3CA exon 20 mutations are associated with poor prognosis in breast cancer patients. Clinics (Sao Paulo), 2012, 67(11): 1285–1290.
[47] Harlé A, Lion M, Lozan N, Husson M, Harter V, Genin P, Merlin JL. Analysis of PIK3CA exon 9 and 20 mutations in breast cancers using PCR-HRM and PCR-ARMS: correlation with clinicopathological criteria. Oncol Rep, 2013, 29(3):1043–1052.

Corresponding author
Nicolae Mirancea, Professor, PhD, Head of Department of Plant and Animal Cytobiology, Institute of Biology Bucharest of Romanian Academy, 296 Independenţei Avenue, P.O. Box 56–53, 060031 Bucharest, Romania; Phone +4021–221 92 02, Fax +4021–221 90 71, e-mail: nick_mirancea@yahoo.com

Received: March 9, 2015

Accepted: December 30, 2015